Using the Cosmic Ray Muon Detector as an Ionizing Radiation Detector

Edward Jin
MIT Department of Physics
(Dated: April 26, 2022)

By sampling a wide variety of radioactive sources, the Cosmic Ray Muon Detector was found to be effective at estimating radioactive activity of medium-energy and medium-activity γ sources, as well as in giving an approximation of particle energy. Further, we show that the detector can verify various known properties of radioactivity, including its Poissonian nature, the randomness of decays, and the theoretical $\frac{1}{r^2}$ relationship between distance and radioactivity. The $\frac{1}{r^2}$ relationship is further confirmed with a Monte Carlo simulation of radioactive decay.

I. INTRODUCTION

Cosmic rays constantly bombard the Earth and can induce radioactive decays, producing muons about 15 km above the Earth's surface. While muons have a lifetime of only 2.2 µs, high-energy muons experience significant time dilation and be detected on Earth. The muons that hit the Earth have mean energy 4 GeV, and can be detected by the Cosmic Ray Muon Detector (CRMD), as described in [1].

The CRMD also detects other background radiation events, thus obscuring the muonic signal. As a result, the CRMD is often used in *coincidence mode*, where two CRMDs are connected together and only record counts when both detectors detect radiation within a short timeframe. Theoretically, low-energy α and β radiation is effectively screened by the detector casing, while γ radiation would undergo Compton scattering and most likely only hit one detector. Thus, in coincidence mode, the counts recorded are almost all from muons.

As the internal apparatus of the CRMD (described in Sec. II) is agnostic between muons and other types of radiation, the CRMD can theoretically also be used as a general-purpose ionizing radiation detector. Non-muonic radioactive decays could potentially pass through the CRMD scintillator, causing an event to be recorded by the CRMD. Thus, putting the CRMD next to a radioactive source can confirm its applicability to radioactive detection.

It is known that radioactive decay can be modeled by a Poisson point process with some decay rate λ unique to each radioisotope. Each radioisotope has a characteristic *half-life*, equal to $\frac{\ln(2)}{\lambda}$, which gives the average time for a sample of N atoms to decay to $N/2$ atoms. Further, by assuming that the radioactive decays 0 in a uniformly random direction, the radiation incident on a detector would be roughly proportional to $\frac{1}{r^2}$, where r is the distance from the detector. All of these properties of radiation can theoretically be verified with the CRMD.

II. EXPERIMENTAL SETUP

The CRMD is a small tabletop device that includes a 5 cm × 5 cm × 1 cm organic plastic scintillator, which is able to extract some energy from high-energy particles and convert it to visible light. When energetic particles pass through a scintillator, some of the energy is deposited in the scintillator, and is captured by a primary fluorescing agent. This primary fluorescing agent can then convert the incident energy to a proportional amount of UV light, which a secondary fluorescent agent can absorb and release a proportional amount of visible light. In the CRMD, various phenyloxazoles are used as fluorescing agents inside the scintillator, and the resulting scintillator has maximum emission wavelength around 420 nm. The light emitted is then detected with the MicroFC 60035 C-Series silicon photomultiplier, which converts the light to an electrical signal that is ultimately processed by a Arduino microcontroller.

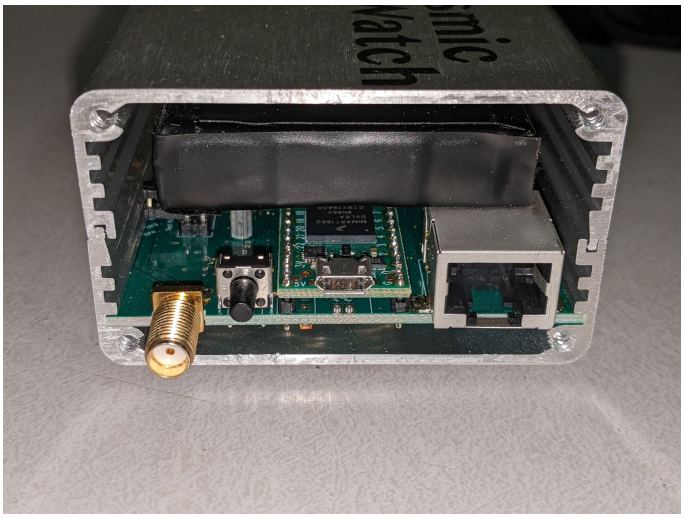

FIG. 1. A cutaway view of the CRMD. The scintillator is connected to a photomultiplier, and both components are first wrapped in aluminum foil to reflect photons, and then in 2-3 layers of black electrical tape to minimize ambient light pollution, as seen above.

To measure muonic radiation, two CRMDs operating in coincidence mode were stacked on top of each other inside the MIT Junior Laboratory and were left to collect data for approximately 2 days. To measure radioactivity, one CRMD was first roughly enclosed in lead bricks to reduce background effects, and various radioisotopes (see

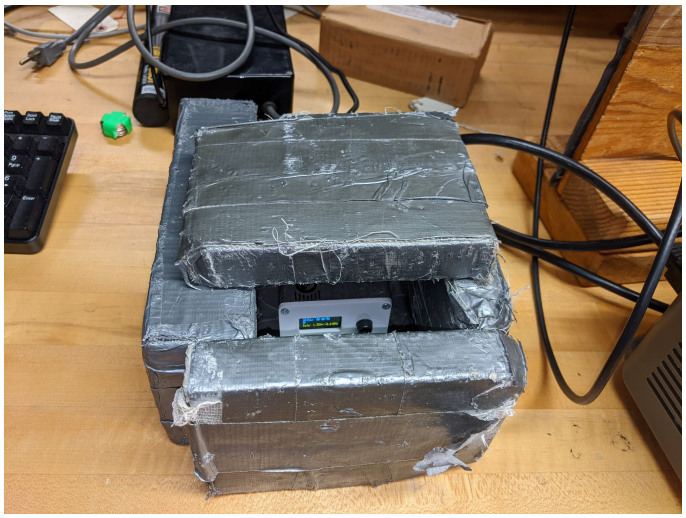

FIG. 2. The CRMD in a lead enclosure in the Junior Laboratory. This setup was used to measure the activities of various radioisotopes listed in Table I.

Isotope/Decay	Date Received	Activity	Rate	Half Life
^{238}U, γ	Apr. 1986	$\approx$ 100 µCi	$>$ 3500 Hz	long
^{60}Co, γ	Jun. 2010	10 µCi	300 Hz	5.3y
^{22}Na, γ	Aug. 2014	10.6 µCi	170 Hz	2.6y
^{90}Sr, β	Feb. 1979	1 mCi	18 Hz	29y
^{241}Am, α	Apr. 1984	10 mCi	3.2 Hz	long
^{55}Fe, γ	Apr. 1986	20 mCi	1.4 Hz	2.7y
^{137}Cs, γ	Nov. 1994	7.7 µCi	180 Hz	30y
^{60}Co, γ	Nov. 1994	0.9 µCi	5.3 Hz	5.3y
^{133}Ba, γ	Nov. 1994	6.6 µCi	4.0 Hz	11y
^{22}Na, γ	Nov. 1994	7.6 µCi	2.0 Hz	2.6y
^{109}Cd, γ	Apr. 1995	7.9 µCi	1.5 Hz	1.3y
^{54}Mn, γ	Mar. 1995	7.4 µCi	1.5 Hz	0.9y
^{57}Co, γ	Mar. 1995	7.8 µCi	1.4 Hz	0.7y
Background	-	-	1.4 Hz	-

TABLE I. Various Measured Radioisotopes. The activities listed are those measured at date of receipt. No activity or isotopic labelling was recorded for the Uranium source, so the activity was calculated according to the listed mass of 342 g UO_2 and assuming 100% ^{238}U. The ^{238}U count rate was too high for the detector to handle; only a lower bound is listed. All count rates are ±10%.

Table I) were placed directly in front of the CRMD. Finally, to measure the distance-dependence of radioactivity, a 1-pound cylindrical container of ^{40}K was suspended from the ceiling, and a CRMD was incrementally moved upwards to vary the distance. All detection data was recorded on local CRMD SD cards and later analyzed with computer.

III. EXPERIMENTS AND RESULTS

III.1. Rate Measurements and Count Distribution

First, we measured the rates of various radioactive sources, which is tabulated in Table I. The first set of radioisotopes consisted of those with a variety of emission features, allowing us to test the limits of the detector. The second set of radioisotopes comes from gamma radiation test kits, where all sources were sealed into the same shape. As the laboratory contained two test kits, sources from both were measured, and the averaged rates and activities are shown in the table. As these radioisotopes were only measured for a few minutes at a time, the statistical uncertainties are quite high. A rate uncertainty of 10% was crudely estimated from the comparison of rates between the sources in the two test kits, and taken as a baseline uncertainty for all rate measurements.

From the ^{238}U data, we see an inherent limit in the detector: it was not designed for high-radiation sources, and hence cannot accurately measure their rates. During measurement, the CRMD also crashed if it was reset next to the source itself, and the rate was continuously increasing every time the display updated. The dead time was over 92% of the total time.

More information about the type of incident radiation it detects can be obtained from the ^{241}Am, ^{90}Sr, and ^{55}Fe data. Despite the high activities of each of these sources, the CRMD only sees minor increases in the rate. ^{90}Sr decays purely via β-decay, and the noticeable but much-lower-than-expected change in rate indicates that the casing of the CRMD is effective at filtering out β-decay events. ^{241}Am has high-energy α-decays, but like the ^{90}Sr, fails to cause a large change in CRMD rate as expected, indicating that the device is even more effective at filtering out α-decays. Finally, ^{55}Fe decays with a gamma-ray of only 5 keV, and causes no noticeable change in the CRMD rate as compared to background. This is despite a very high initial activity and a sufficiently long half life, leading to the conclusion that low-energy γ radiation also is not detected by the CRMD. Thus, given these samples, we conclude that the CRMD can work as a radiation detector, but is limited in that it cannot effectively detect α, β, or low-energy radiation, and also cannot handle high-radiation environments.

The results of the gamma-ray test kits give some measure of accuracy of detection. For the three isotopes ^{109}Cd, ^{54}Mn, ^{57}Co, the detector detects nothing significant above background. This makes sense, given that roughly 20-30 half-lives have passed, leading to sub-becquerel activities and an even lower proportion that hit the detector. Aside from ^{133}Ba, the isotopes that still give a signal have similar ratios of calculated activity to their measured activity, as in Fig. 3, indicating that the CRMD is sufficient at giving an approximate radioactive count rate. ^{133}Ba has activity noticeably lower than predicted; we hypothesize that this is due to the low-energy of its emissions (its primary emission is at 31 keV, followed by 356 keV as the secondary emission), resulting in a lower-than-expected incidence rate on the detector. This failure at low energy is expected, given that ^{55}Fe also gave no appreciable counts earlier.

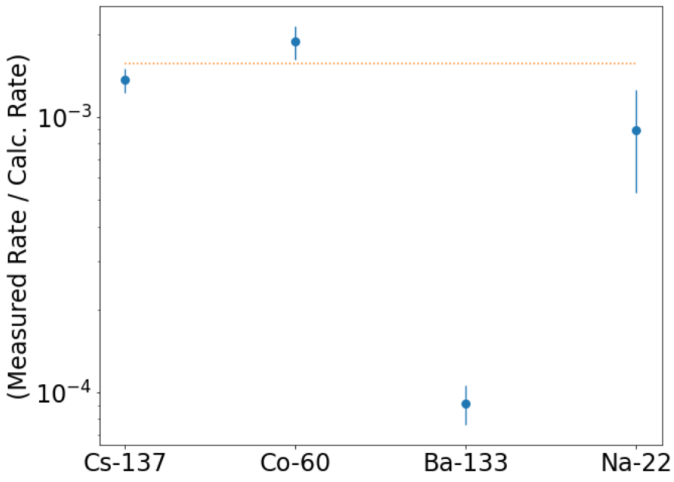

FIG. 3. The ratio of calculated count rate to measured count rate. As the tubes had the same shape, the ratio of events reaching the detector should be roughly constant, meaning that the ratio of calculated rate to measured rate should also be constant. Excluding the ^{133}Ba, a constant fit to the data yielded a χ^2 value of 5.27, with corresponding probability $P(\chi^2 > 5.27; df = 2) = 7\%$.

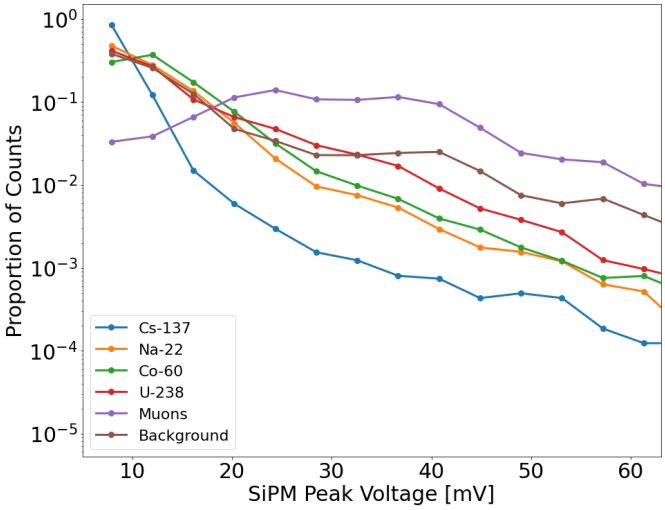

FIG. 4. The proportion of counts that fall within a SiPM voltage range. To have pure signals, only high-count rate radioisotopes, which would drown out the background signal, were plotted. In addition, background and muonic data can be separated with CMRDs operating in coincident mode, and are plotted as well.

III.2. Energy Dependence

The silicon photomultiplier (SiPM) voltage is roughly proportional to how much energy the scintillator actually absorbed. As a result, measuring the SiPM reading should theoretically give some proxy of incident energy. However, the energy an incoming particle deposits can range from 1% (in the case of muons), to 100% of its original energy, making it hard to assign actual particulate energies to voltages. Further, the resolution of the CRMD is nowhere as precise enough as needed for the actual recording of spectra, as seen in Fig. 4. However, some interesting information can still be gleaned from the SiPM data.

First, the muonic signal clearly behaves differently than the radioactive signals, in that the proportion of events is relatively constant across the SiPM voltage range. In addition, its peak is not at the lowest SiPM peak voltage, unlike the other radioactive events. This confirms that muonic energies are much higher than those of the radioisotopes and have a different distribution.

Second, the tails of the distribution seem to give an approximate measure of incident energy. From Fig. 4, we see that the ordering of tails is ^{137}Cs $<$ ^{60}Co $\approx$ ^{22}Na $<$ ^{238}U. This ordering matches with known energy data: 0.66 MeV for ^{137}Cs, 1.17 and 1.33 MeV for ^{60}Co, 1.28 MeV for ^{22}Na, and 1.76 MeV for ^{238}U (most prominent). The background distribution has an even bigger tail; we hypothesize that this is because background radiation partially comes from ^{222}Rn, which has the same 1.76 MeV gamma ray as ^{238}U, but with it being a significantly higher proportion of the total ^{222}Rn radioactivity.

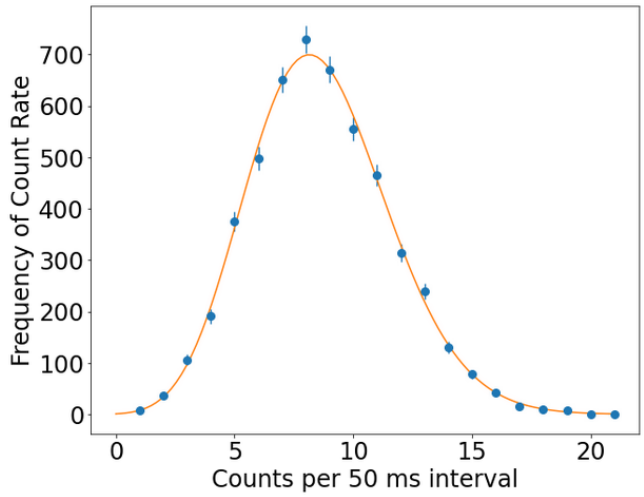

FIG. 5. The frequency of the number of counts in each 50-ms interval for ^{22}Na. Fitting a Poisson distribution to the data yielded a χ^2 value of 15.6, with corresponding probability $P(\chi^2 > 15.6; df = 19) = 68\%$.

III.3. Randomness of Radioactive Decays

As shown in previous work [2], muonic decay follows a Poisson distribution, and this result can be shown with the CRMD. To verify this for radioisotopes as well, we chose to analyze the high-activity ^{22}Na sample. By splitting the data into 50-ms intervals and plotting the frequency of count occurrence, we expect a Poisson distribution, as the number of counts within each interval is Poisson. This is exactly what we see, as in Fig. 5.

To quantify the randomness of radioactive decay beyond its Poissonian nature, we first created a random bitstream from the ^{22}Na data, by converting the parity of the timestamp to binary bits. We then performed two randomness tests on the data: an 8-substring test, and a 5×5 binary rank test.

The 8-substring test works by generating all possible substrings of 8 bits, and then seeing the frequency of each binary string appearing. For a truly random generator, the frequency of each substring should be uniform. This is indeed what is observed in the data, when comparing to the uniform distribution $[\chi^2 = 302, P(\chi^2 > 302; df = 255) = 2.3\%, N = 44316]$.

The binary rank test splits the bitstream into independent 25-length bitstrings, which are then reshaped into a 5×5 matrix. The matrix rank should then follow the rank distribution of a completely random 5×5 binary matrix, which can be calculated via brute force. By using independent strings of 25 bits from the bitstream, a rank distribution was calculated and found to be similar to the expectation $[\chi^2 = 3.2, P(\chi^2 > 3.2; df = 6) = 78\%, N = 1772]$. As both randomness tests pass, radioactive decay times are likely to be random, as expected.

III.4. Distance Dependence of Radioactivity

To calculate the distance dependence of radioactivity, the CRMD was placed at 12 varying heights relative to a container of natural potassium chloride. The CRMD recorded count rates ranging from 1.46 Hz (background), all the way to 3.41 Hz (container placed directly on top of detector). The experimental data uncertainties were estimated to be 3%, based on [2] and a 1% distance measurement uncertainty.

In order to quantitatively estimate the distribution of radioactive decay, we performed an MC simulation of the radioactive decays in Python. Using a precision caliper, various aspects of the apparatus, including KCl container radius and height, detector position, and detector area, were measured. Further, a known value for the attenuation constant of KCl of 0.0584 was used to simulate self-absorption [3].

The simulation chooses a random point in the KCl container, and then chooses a random direction for the radiation to propagate. If the chosen direction eventually intersects the detector, the detector then has a probability of $e^{-\mu d}$ of triggering an event, where μ is the attenuation coefficient and d is the distance travelled within the container. For each condition, $5 \cdot 10^6$ points are simulated, and their average hit rate is the output of the simulation. This number of points was sufficient to give consistent simulation results within 1% statistical uncertainty.

The MC simulation systematic uncertainties were estimated, by varying parameters within 1σ, to be 4%. Multiplying by a normalization factor, representing the proportion of decays that actually trigger the detector, then gives the computed rate from the MC simulation. This normalization factor was obtained by performing a linear fit between the MC rates and measured rates.

We then fit a scaled inverse square law to the MC data, which to our surprise, fit essentially perfectly. This meant radioactive decay is still expected to follow an inverse square law, even in our nonideal system. We also find good agreement between the experimental data and the MC simulation / inverse square law, as shown in Fig. 6.

IV. CONCLUSION

Overall, we performed a diverse set of experiments with the CRMD to evaluate its capabilities for measuring radiation. We found that it does well with medium-energy medium-activity γ sources, while it is unable to detect α, β, and low-energy radiation effectively. We then use the CRMD to verify known properties of radioactivity, including its random Poisson nature and $\frac{1}{r^2}$ dependence.

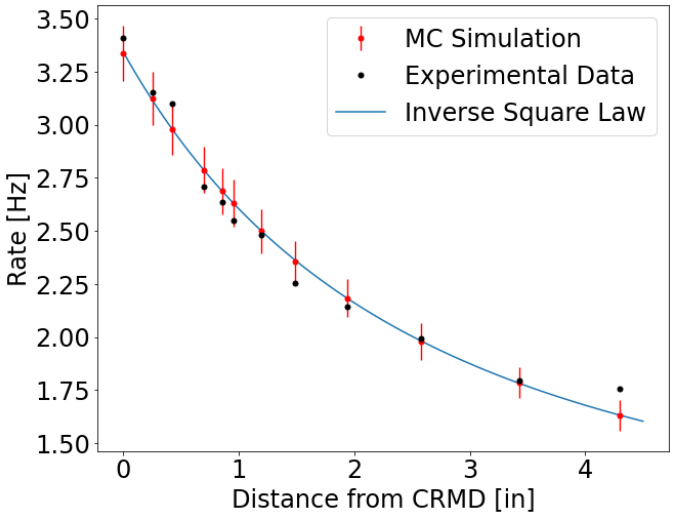

FIG. 6. The inverse square law accurately captures the rate predictions of the MC simulation. The MC systematic uncertainty was estimated to be 4%. The experimental data matches with the inverse square law and MC simulation, with $\chi^2 = 12.6, P(\chi^2 > 12.6; df = 8) = 13\%$.

[1] S. N. Axani, "The physics behind the cosmicwatch desktop muon detectors," (2019), arXiv:1908.00146 [physics.ins-det].

[2] E. Jin, "Cosmic ray muon detector analysis," (2022), unpublished (submitted on Canvas; Written Summary 0).

[3] S. Gowda, International Journal of Physical and Mathematical Sciences **10**, 392 (2016).